

Dynamical formation and interaction of bright solitary waves and solitons in the collapse of Bose–Einstein condensates with attractive interactions

B J Dąbrowska-Wüster^{1,2,5}, S Wüster^{3,4} and M J Davis¹

¹ ARC Centre of Excellence for Quantum-Atom Optics, School of Mathematics and Physics, The University of Queensland, QLD 4072, Australia

² Institute of Natural Sciences, Massey University Albany, North Shore MSC, 0745 Auckland, New Zealand

³ School of Mathematics and Physics, The University of Queensland, QLD 4072, Australia

⁴ Max Planck Institute for the Physics of Complex Systems, Nöthnitzer Strasse 38, 01187 Dresden, Germany

E-mail: b.dabrowska-wuester@massey.ac.nz

New Journal of Physics **11** (2009) 053017 (15pp)

Received 24 November 2008

Published 27 May 2009

Online at <http://www.njp.org/>

doi:10.1088/1367-2630/11/5/053017

Abstract. We model the dynamics of formation of multiple, long-lived, bright solitary waves (BSWs) in the collapse of Bose–Einstein condensates with attractive interactions as studied in the experiment of Cornish *et al* (2006 *Phys. Rev. Lett.* **96** 170401). We use both mean-field and approximate quantum field simulation techniques. While a number of separated wave packets form as observed in the experiment, they do not have a repulsive π phase difference as has been previously inferred. We observe that the inclusion of quantum fluctuations causes soliton dynamics to be predominantly repulsive in one-dimensional (1D) simulations independent of their initial relative phase. However, indicative 3D simulations do not show a similar effect. In contrast, in 3D quantum noise has a negative impact on BSW lifetimes. Finally, we show that condensate oscillations, after the collapse, may serve to deduce three-body recombination rates.

⁵ Author to whom any correspondence should be addressed.

Contents

1. Introduction	2
2. 3D BEC collapse	4
3. 1D collapse with quantum noise	7
4. Quantum soliton collisions	8
5. 3D BSW collisions	11
6. Conclusions	12
Acknowledgments	13
References	13

1. Introduction

At low temperatures it is well known that the wavefunction of an interacting Bose–Einstein condensate (BEC) can be described by solutions of the nonlinear Gross–Pitaevskii equation (GPE) for both repulsive and attractive atomic interactions [1]. In a one-dimensional (1D) system a BEC with intrinsic attractive interactions can form localized states for any number of particles. These are known as bright matter-wave solitons, and demonstrate particle-like behaviour in collision events [2]. Single and multiple bright matter-wave solitons have been observed in a quasi-1D geometry through the tuning of atomic interactions from repulsive to attractive in a ^7Li condensate with a Feshbach resonance [3, 4]. A bright soliton was also observed by Eiermann *et al* by rendering the effective mass of a repulsive ^{87}Rb condensate negative by applying a 1D optical lattice [5].

Corresponding soliton solutions for condensates with attractive interactions are not possible in free space in 3D. However, for a harmonically trapped BEC, a condensate wavefunction can be found for particle numbers less than a critical value N_{cr} [6]. Condensates with a particle number exceeding this value are unstable against collapse as demonstrated in the Bosenova experiment at JILA [7] and previously at Rice University [4, 8, 9]. Bright solitary wave (BSW) solutions to the 3D GPE with moderately tight harmonic trapping in 2D can be found for a condensate with attractive interactions as demonstrated by Parker *et al* [10, 11]. These are analogous to the soliton solutions of the 1D GPE, but are only self-trapped in 1D. The formation and collisions of apparent multiple BSWs in condensate collapse have been observed recently by Cornish *et al* [12].

In the Rice and JILA experiments, repulsive interactions between neighbouring solitons have been inferred directly from the soliton trajectories [4, 12], as well as indirectly as a consequence of the condensate atom numbers remaining in excess of N_{cr} . The long-time evolution of soliton trains [13]–[15] can qualitatively be accounted for by assuming that neighbouring solitons have a *repulsive* phase difference $\Delta\varphi$. In mean-field theory this implies $\pi/2 < \Delta\varphi < 3\pi/2$ [16]. However, the *development mechanism* of a repulsive phase-relation between the soliton-like structures in the experiments has not been explained.

In this work, we make an attempt to understand the physics of the formation of 3D BSWs in condensate collapse, by using mean-field and quantum dynamical simulation methods incorporating the effects of three-body loss. We focus on modelling the results of the experiment by Cornish *et al* [12], who caused an initially stable ^{85}Rb condensate to collapse by switching

the inter-atomic interaction from repulsive to attractive using a Feshbach resonance [17] while keeping the trapping potential on. At this point the number of atoms in the condensate exceeds the critical atom number for stability, N_{cr} , which causes the macroscopic wave function to collapse [7], [18]–[20], in the process losing atoms due to three-body recombination. As was found in earlier experiments, the onset of loss is sudden, and this allows the precise definition of the collapse time, t_{collapse} [7], which is largely independent of the three-body recombination rate [7, 18, 19]. Following this primary collapse, it might be expected that repeated collapse processes and subsequent loss occur until the atom number decreases below the critical value, N_{cr} [21]. In contrast, experiments [7, 12] have reported remnant atom numbers, N_{remn} , several times larger than N_{cr} even after long evolution times. In [12], this is attributed to the creation of multiple bright solitons with mutual repulsive phase differences preventing any further collapse of the condensate. Parker *et al* have studied the collisions of 3D BSWs for the conditions of the experiment of Cornish *et al* [12] in mean-field theory as a function of relative phase and velocity [10, 22]. They have found that while the survival of the BSWs requires a repulsive relative phase at low velocities, for sufficiently large relative velocity the BSWs survive single collision events independent of the relative phase. They also found that a $\Delta\varphi$ in the repulsive range can inhibit collapse-induced destruction of the soliton pair for many oscillation periods involving more than 40 collisions [10, 22].

In this article, we begin by modelling the initial collapse and structure formation of the experiment of Cornish *et al* [12] by solving the mean-field GPE in 3D with realistic parameters. We find that the dynamical *creation* of solitons as in [12] does *not* favour repulsive $\Delta\varphi$. For the Rice experiment [4], the absence of fixed repulsive phase-relations in Gross–Pitaevskii (GP) simulations of soliton creation was pointed out in [23]. For the JILA experiment [12], the fact that the initial GP wave function has even symmetry prevents repulsive phase relations in the final state for an even number of BSWs as mean-field theory preserves this symmetry. In this situation, the central two members of the train must therefore have $\Delta\varphi = 0$. In order for this statement to be false, there must be some form of symmetry-breaking mechanism.

To go beyond mean-field theory, we next account for quantum field corrections to the GPE by modelling the collapse using the truncated Wigner approximation (TWA) [24]–[26] which incorporates the effects of quantum noise. However, we find that for conditions close to the experiment [12] the relative phase between the central two dynamically formed BSWs is still near zero. An example of BSWs with attractive phase relations found within truncated Wigner quantum field theory is shown in figure 1.

In order to better understand the effects of quantum noise in condensate collapse events, we consider the soliton formation in the quasi-1D Rice experiment [4], which has the advantage of being easier to model. We find that quantum fluctuations have a significant effect on the resulting soliton interactions. We then perform controlled collisions between solitons of varying relative phase in 1D, and find that quantum noise tends to render soliton interactions more repulsive than the corresponding mean-field solution, *irrespective* of their relative phase.

Finally, we perform indicative 3D simulations that suggest N_{remn} can remain above N_{cr} for long times in the presence of quantum and thermal fluctuations even if the interactions of the corresponding mean-field BSWs are attractive. We find, however, that the effects of quantum noise tend to destroy the BSW structures for all initial relative phases, in contrast to the results of mean-field simulations [10, 22] and experiment [12].

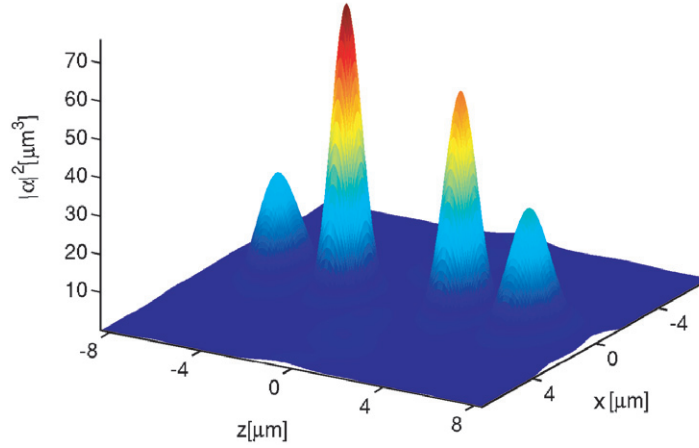


Figure 1. Dynamically formed 3D matter-wave BSWs (close-up of atom density cross-section for $y = 0$). Simulations using truncated Wigner quantum theory for $a_{\text{collapse}} = -20a_0$ and $K_3 = 5 \times 10^{-38} \text{ m}^6 \text{ s}^{-1}$. The snapshot is taken 16 ms after the collapse.

In summary, we report two important results. Firstly, the inference that the BSWs observed in [12] have repulsive relative phases is in disagreement with GP theory and does not find any support in the approximate quantum field simulations that we can perform. Secondly, our study of the 1D analogue of this experiment (which is more tractable computationally) indicates that quantum fluctuations can render soliton interactions repulsive regardless of their relative phase. We have no evidence to suggest that this is the correct interpretation of the experiments [4, 12], and indeed our indicative 3D simulations do not support this hypothesis. However, we hope that by highlighting these problems we will motivate further experimental and theoretical research on this topic.

2. 3D BEC collapse

We first model collapsing condensates using the time-dependent GPE

$$i\hbar \frac{\partial}{\partial t} \Phi = \left(-\frac{\hbar^2}{2m} \nabla^2 + \frac{1}{2} m (\omega_r^2 r^2 + \omega_z^2 z^2) + g |\Phi|^2 - i \frac{\hbar}{2} K_2 |\Phi|^2 - i \frac{\hbar}{2} K_3 |\Phi|^4 \right) \Phi, \quad (1)$$

with phenomenological two- and three-body loss terms [18, 21, 27]. Here the condensate wave function $\Phi(r, z)$ is written in cylindrical co-ordinates. We assume ^{85}Rb atoms with mass $m = 1.411 \times 10^{-25} \text{ kg}$, interaction strength $g = 4\pi \hbar^2 a_s(t)/m$, where the scattering length $a_s(t)$ varies in time. We define $a_s(t=0) = a_{\text{ini}} \geq 0$ and $a_s(t > 0) = a_{\text{collapse}} < 0$. Further, $\omega_r/2\pi = 17.3 \text{ Hz}$ and $\omega_z/2\pi = 6.8 \text{ Hz}$ [12]. The three-body loss rate, K_3 , has not been precisely determined for the conditions of [12]. For this reason, and for numerical necessity, we vary K_3 throughout this work. We take $K_2 = 1.87 \times 10^{-20} \text{ m}^3 \text{ s}^{-1}$ [28]. Our initial condition is the solution to the time-independent GPE with $a_s = a_{\text{ini}}$ found via imaginary time evolution. To reduce the computational demands of the problem, we use a spatial grid size that does not

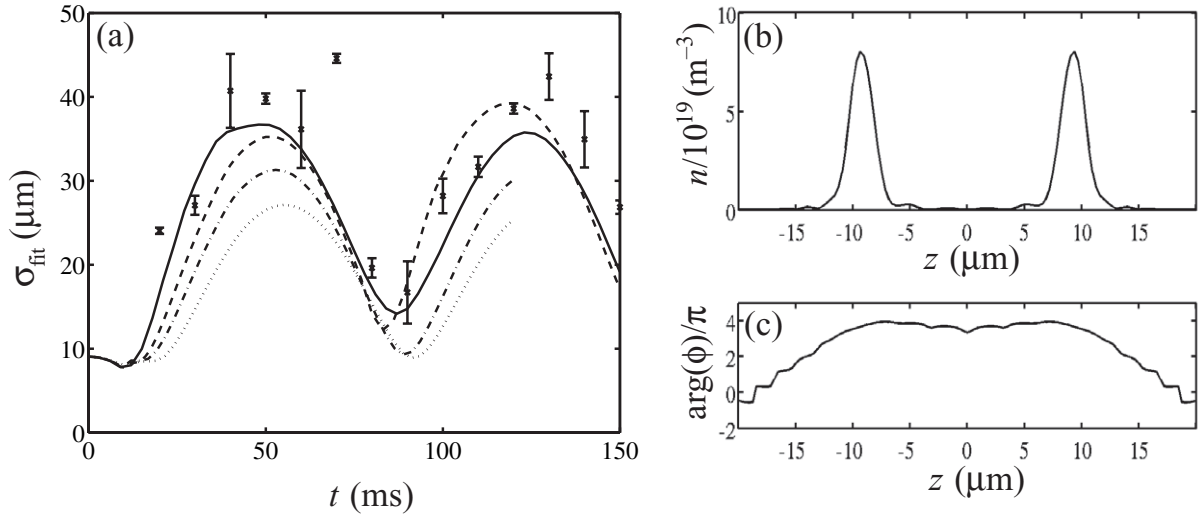


Figure 2. 3D mean-field simulations of dynamically formed BSWs compared with experimental data from [12]. (a) Full-width half-maximum (FWHM) in the z -direction calculated for $a_s = -11.4a_0$ and $K_3 = 0.2 \times 10^{-39} \text{ m}^6 \text{ s}^{-1}$ (solid line); $K_3 = 1 \times 10^{-39} \text{ m}^6 \text{ s}^{-1}$ (dashed); $K_3 = 4 \times 10^{-39} \text{ m}^6 \text{ s}^{-1}$ (dotted–dashed); $K_3 = 16 \times 10^{-39} \text{ m}^6 \text{ s}^{-1}$ (dotted). Experimental points as in figure 3 of [12] are shown with (\times). For all results, a 2D Gaussian function is fitted to the experimental and numerical column densities using a least squares method. (b) Density and (c) phase of the condensate along the z -axis at the time $t = 75 \text{ ms}$.

fully accommodate burst atoms ejected during collapse [7]. As these are not the focus of our studies, we employ absorbing potentials near all numerical grid edges⁶.

In figure 2, we compare our numerical solutions of (1) with the experimental data from [12] for the case $a_{\text{collapse}} = -11.4a_0$ and $a_{\text{ini}} = 9a_0$, where a_0 is the Bohr radius. For these initial conditions, the experiment observes the formation of two BSW-like structures. We solve (1) in cylindrical co-ordinates using a Fourier transform-based adaptive step-size Runge–Kutta algorithm. The collapse time [7] for this scenario is $t_{\text{collapse}} = 12 \text{ ms}$. Near this time the peak density rises dramatically with a maximal value that scales as U/K_3 [29]. Directly after the collapse burst atoms are ejected from the condensate⁷. The so-called burst focus [7] takes place at a later time, when all ejected atoms that did not hit the absorber have classically completed half of an oscillation in the radial potential and have returned to the trap symmetry axis. This happens at $t_{\text{bf}} = t_{\text{collapse}} + \pi/\omega_r \approx 41 \text{ ms}$. We see the onset of the burst focus around 35 ms. The burst focus develops into two axially separate clouds, in agreement with experimental observations [30]. In our simulations these become precursors of a BSW pair. It takes until $t = 72 \text{ ms}$ before these clouds develop two distinct BSW-like shapes. The distance by which the atoms are axially displaced by the collapse, and hence the width found in figure 2, increases for lower K_3 due to the larger interaction energy that is

⁶ The absorbers have the generic form $V_{\text{damp}} = i\gamma(1 - \cos[\pi(d - \Delta x)/d])\theta(d - \Delta x)$, where Δx is the distance to the nearest grid edge, d the absorber width, θ the Heaviside step function and γ is the absorber strength.

⁷ In our simulations most of these are eliminated with the absorbing potential.

liberated during the collapse. Beyond $t \sim 50$ ms the absorbing potentials become relevant for the dynamics.

It is generally expected that the atom bursts have a strong uncondensed component [31, 32], which in principle necessitates a theoretical treatment beyond the mean-field for $t > t_{\text{collapse}}$. The numerical results in figure 2 obtained using GP theory are hence approximate. Nonetheless, they describe the initial evolution of the experimentally observed FWHM rather well. Furthermore, the amplitude of the condensate oscillations depends strongly on the three-body loss rate K_3 and the agreement between theory and experiment is better for smaller K_3 . We suggest that this may allow for a better experimental measurement of K_3 than has been possible so far [28]. The reliability of this approach would depend on the influence of the uncondensed burst atoms. Most importantly, we confirm that the BSWs are created *in-phase* as required by symmetry.

We now consider the effect of quantum fluctuations on the collapse. It has been suggested that quantum fluctuations can imprint a staggered phase pattern onto the condensate cloud during the development of instability [14]. To investigate this we employ the TWA [20], [24]–[26], [33] of the full quantum evolution of the condensate. In this approach, quantum field effects enter through the rigorous addition of noise to the initial condensate wave function. Assuming an initial coherent state for the atomic quantum field, we begin our simulations with the stochastic field

$$\alpha(\mathbf{x}, t = 0) = \Phi(\mathbf{x}, t = 0) + \frac{1}{\sqrt{2}} \sum_n \varphi_n(\mathbf{x}) \eta_n. \quad (2)$$

Here $\Phi(\mathbf{x}, t = 0)$ is the condensate initial state as used in mean-field simulations, $\varphi_n(\mathbf{x})$ are the computational basis states and η_n is a complex Gaussian random noise with correlations $\overline{\eta_n \eta_m} = 0$, $\overline{\eta_n^* \eta_m} = \delta_{nm}$. The *stochastic field* $\alpha(\mathbf{x})$ then evolves according to (1), which has to be solved for many realizations of the noise in (2). Quantum expectation values involving the atom field $\hat{\Psi}(\mathbf{x})$ can be obtained from stochastic averages (denoted by $\overline{\dots}$) over the ensemble of simulated trajectories [24]

$$\langle \hat{\Psi}^\dagger(\mathbf{x}) \hat{\Psi}(\mathbf{x}) \rangle = \overline{\alpha(\mathbf{x})^* \alpha(\mathbf{x})} - \frac{1}{2\Delta V}. \quad (3)$$

Here ΔV is the volume element associated with a numerical grid point. It can be shown that this prescription reproduces the quantum evolution of the system as long as the noise remains small and times are short [24, 26], [34]–[36]. A physical interpretation of the applied noise is possible—for the initial state (2), the condensate wave function $\Phi(\mathbf{x})$ represents the mean value of the coherent state on the numerical grid point \mathbf{x} , whereas the noise contribution $\sum_n \varphi_n(\mathbf{x}) \eta_n / \sqrt{2}$ gives the appropriate field uncertainty in both amplitude and phase. The evolution of this initial spread in amplitude and phase as the ensemble of trajectories is propagated in time, allows us to determine the quantum dynamics of fluctuations. Since both soliton train experiments used single realizations of the atomic density to infer soliton dynamics, we exclusively consider single realizations of the truncated Wigner quantum noise and not multi-trajectory averages. More details on the truncated Wigner method can be found in the literature [20], [24]–[26], [33]–[35], [37]. In particular, we note the recent extensive review article that provides a full introduction to the TWA for simulations of BECs [36].

For a more accurate treatment of the three-body losses, we optionally include dynamical noise terms in our simulations [38]. The theoretical and numerical methods employed here are described in [20]. The full truncated Wigner equation of motion for the stochastic field is [38]

$$\begin{aligned} d\alpha(\mathbf{x}) = & -\frac{i}{\hbar} \left(-\frac{\hbar^2}{2m} \nabla^2 + V(\mathbf{x}) + U_0 |\alpha(\mathbf{x})|^2 \right) \alpha(\mathbf{x}) dt \\ & - \frac{K_3}{2} |\alpha(\mathbf{x})|^4 \alpha(\mathbf{x}) dt + \sqrt{\frac{3K_3}{2}} |\alpha(\mathbf{x})|^2 d\xi(\mathbf{x}, t), \end{aligned} \quad (4)$$

with dynamical noise $d\xi(\mathbf{x}, t)$ that has correlations $\overline{d\xi(\mathbf{x}, t)d\xi(\mathbf{x}', t')} = 0$, $\overline{d\xi(\mathbf{x}, t)^*d\xi(\mathbf{x}', t')} = \delta(\mathbf{x} - \mathbf{x}')\delta(t - t')$. Here, the cylindrical symmetry is broken by the noise in the initial state (2). For a consistent treatment of the noise, the propagation algorithm uses the harmonic oscillator basis [20, 33]. For the problem to remain computationally tractable in this basis, we increase K_3 compared with the values in figure 2 (see e.g. figure 1), thus sacrificing direct correspondence to the experiment. We also apply the quantum treatment to a low energy subset of the full mode space in order to justify the TWA.

Within these constraints, our quantum field simulations show little difference from the mean-field GPE results—there is no signature of a preference for repulsive $\Delta\varphi$ for a large range of a_{collapse} . Therefore the results of our 3D simulations question the assertion that BSWs originating from a condensate collapse as in [12] are created with a repulsive phase relation between neighbours. In order to more fully understand the effect of quantum noise in BEC collapse events, we now turn to the quasi-1D situation, which is more computationally tractable.

3. 1D collapse with quantum noise

While the investigation of quantum effects in 3D for the realistic experimental parameters of [12] remains computationally intractable⁸, it is possible to gain insight into the effects of quantum noise in a 1D situation. We have therefore performed 1D simulations that can be expected to qualitatively model the soliton formation experiment conducted in an elongated trapping geometry by Strecker *et al* [4]. A full quantitative comparison cannot easily be done as 3D features are expected to be important in the collapse processes themselves [23]. To derive a 1D model, we integrate out the transverse dimension r of (1) for $K_2 = 0$, using the approximation that the system remains in the ground harmonic oscillator state in these dimensions [39]. The resulting 1D GPE incorporating three-body loss is

$$i\hbar \frac{\partial}{\partial t} \Phi = \left[-\frac{\hbar^2}{2m} \frac{\partial^2}{\partial z^2} + \frac{1}{2} m \omega_z^2 z^2 + g_{1D} |\Phi|^2 - i \frac{\hbar}{2} \tilde{K}_{3,1D} |\Phi|^4 \right] \Phi, \quad (5)$$

where $g_{1D} = g/(2\pi a_r^2)$ and $\tilde{K}_{3,1D} = K_3/(3\pi^2 a_r^4)$ with $a_r = \sqrt{\hbar/(m\omega_r)}$.

The experiment [4] used a top-hat-shaped condensate initial state, displaced to the side of a harmonic potential. The centre of mass motion of a condensate in a harmonic trap fully decouples from the relative dynamics [23]. Thus, we can study this scenario

⁸ The strong localization of the condensate at the moment of collapse necessitates a fine numerical grid and the ejected burst atoms require a large spatial grid domain. Additionally, the experimental conclusions stem from BSW behaviour at long time. Altogether these requirements mean that quantum simulations for the precise experimental parameters would be extremely demanding.

by placing the initial ground state into the centre of the trap for numerical simplicity. Figure 3 shows typical simulations of a 1D collapse⁹. Figures 3(a) and (d) are the mean-field GPE solutions. Close inspection of the high density regions reveals soliton-like structures for most times. Their number, however, is not conserved but varies after each collapse event. We find that no fixed repulsive phase-relations form and that the overall system exhibits breathing oscillations with repeated increase of density accompanied by three-body loss whenever solitons closely approach one another.

Applying the dimensionality reduction used above to (4) yields the 1D stochastic differential equation for the truncated Wigner framework

$$d\alpha = -\frac{i}{\hbar} \left[-\frac{\hbar^2}{2m} \frac{\partial^2}{\partial z^2} + \frac{1}{2} m \omega_z^2 z^2 + g_{1D} |\alpha|^2 \right] \alpha dt - \frac{\tilde{K}_{3,1D}}{2} |\alpha|^4 \alpha dt + \sqrt{\frac{9\tilde{K}_{3,1D}}{8}} |\alpha|^2 d\xi(x, t). \quad (6)$$

Figures 3(b) and (e) show a trajectory of a 1D collapse simulation using the TWA with initial and dynamical noise, implemented only on the central half of Fourier space to avoid aliasing and to keep the noise density much lower than the condensate density [34]. A qualitative difference in the dynamics in the presence of vacuum fluctuations can be noticed, compared with the mean-field simulations—the overall dynamics of the solitons is more repulsive (figure 3(b)) leading to a decrease in the overall atom loss (figure 3(c)) due to lower densities at the moments of solitons closest approach. This behaviour is typical for all realizations of noise, although depending on the atom number and three-body loss rate, the qualitative difference in soliton behaviour between GP and TWA simulations may be less striking than shown in the figure.

In the following section, we investigate the phenomenon of noise induced repulsion more closely.

4. Quantum soliton collisions

While we do not find any evidence that quantum noise facilitates the creation of solitons (in 1D) or BSWs (in 3D) with repulsive phase relations during the BEC collapse, our 1D model suggests that the noise strongly affects the collisional dynamics of the observed solitons. Strong effects of incoherence on the interaction properties of solitons are known from nonlinear optics [40, 41].

To understand this in more detail, we focus on the collision stage and investigate the effect of quantum noise on the interactions of analytically prepared bright solitons. For this we make equation (5) dimensionless with energy, time and length scales given by $\hbar\omega_r$, ω_r^{-1} and a_r , respectively, and set $\tilde{K}_{3,1D} = 0$. The initial state of these 1D simulations is a superposition of a pair of separated bright solitons, individually multiplied by a phase factor $e^{ik_n x}$ such that the solitons propagate towards one other with equal speed. Explicitly

$$\Phi(x, t = 0) = A \sum_{n=1,2} \text{sech}[\gamma(x - p_n)] e^{i(k_n x + \varphi_n)}, \quad (7)$$

with $A = 20$, $\gamma = \sqrt{|\tilde{g}|} A$, $p_{1,2} = \pm 10$, $k_{1,2} = \mp 1$ and $\varphi_1 = 0$. Within mean-field theory the character of the ensuing collision is determined by the independent parameter of relative phase $\Delta\varphi = \varphi_2$. The density evolution for $\Delta\varphi = 0$ ($\Delta\varphi = \pi$) is shown in figure 4(c) (figure 4(d)).

⁹ We refer to a 1D collapse as the situation where narrow density spikes have developed and then exploded due to the onset of strong losses. Unlike the corresponding situation in 3D, a 1D collapse does not develop a mathematical density singularity.

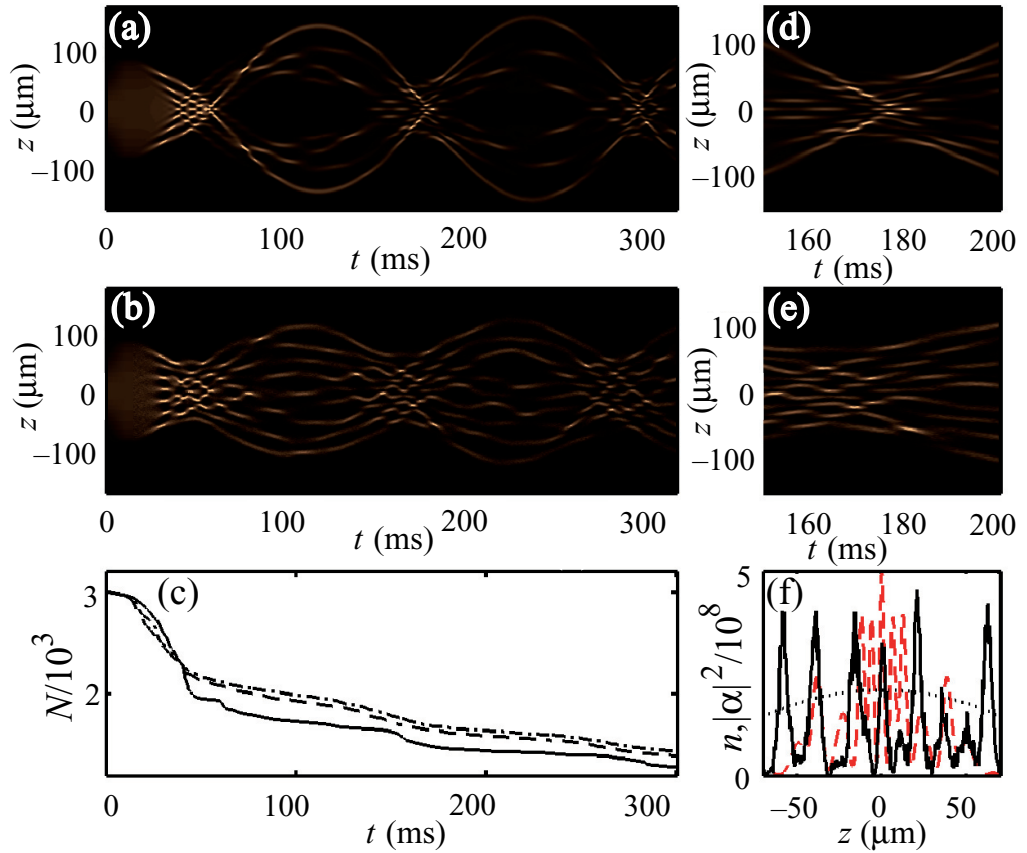


Figure 3. Time evolution of the atomic density (a, b, d–f) and atom number (c) in a 1D harmonic trap. The scenario mimics soliton train creation experiments in lithium [4]. We start from an initial total number of $N_{\text{ini}} = 3 \times 10^4$ atoms in the top-hat shaped ground state of a harmonic trap combined with Gaussian end-caps ($a_{\text{ini}} = 5a_0$). The atoms are then exposed to an attractive nonlinearity with $a_{\text{collapse}} = -3a_0$. Other parameters are $\omega_z/2\pi = 4$ Hz, $a_r = 1.35 \mu\text{m}$ ($\omega_r/2\pi = 800$ Hz) and $K_3 = 3.28 \times 10^{-39} \text{m}^6 \text{s}^{-1}$. Bright (dark) regions correspond to high (low) atomic density. We truncate the density scale at 10% of its peak value to improve visualization. Shown are densities from (a) mean-field theory; (b) TWA. Panels (d) and (e) show close-ups of the first overall contraction around 170 ms. Panel (f) shows the 1D GP density, n (red-dashed), in comparison with the stochastic density, $|\alpha|^2$ (black-solid) at $t = 160$ ms. The black-dotted line is the initial density. The atom numbers in panel (e) are from mean-field theory (solid line), TWA with initial noise only (dashed line) and TWA with dynamical noise (dot-dashed line) with the noise contribution to the atom number subtracted for the truncated Wigner results.

The most significant difference between collisions with opposite relative phase occurs at the moment of closest approach of the solitons, which is labelled by t_* . The solitons merge into a single peak for $\Delta\varphi = 0$, while for $\Delta\varphi = \pi$ they preserve a double peak structure.

Figures 4(a) and (b) show a Gaussian fit to the overall density profile at the time of collision, giving a quantitative criterion to distinguish the attractive and repulsive situations.

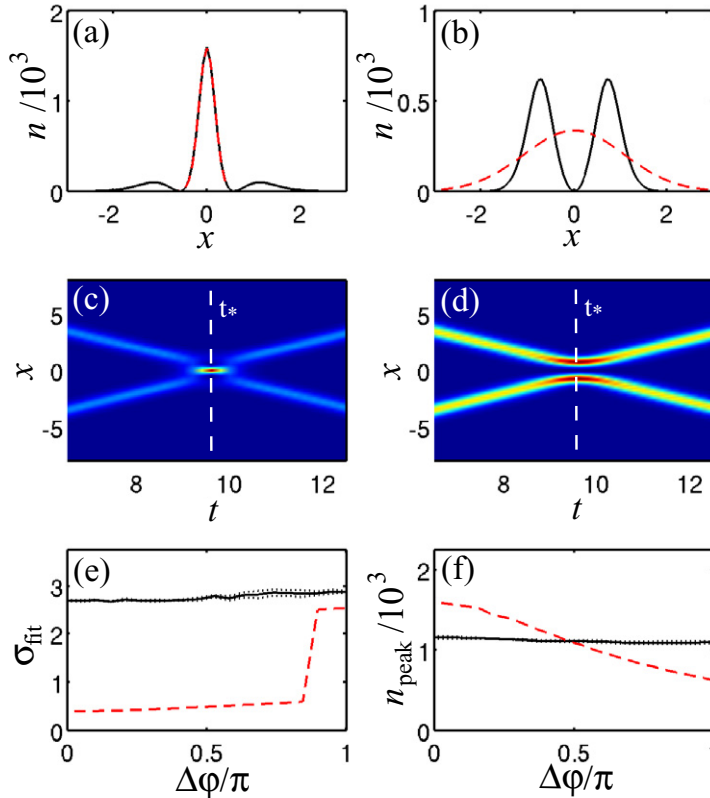


Figure 4. Binary interactions of bright solitons in conservative mean-field and truncated Wigner models quantified by the FWHM in the longitudinal, z , direction. Upper panels: spatial soliton profiles (black-solid) and the Gaussian fit (red-dashed) at time of closest approach, t_* , for $\Delta\phi = 0$ (a) and $\Delta\phi = \pi$ (b). Middle panels: close-ups of time evolution of soliton densities (red highest, blue lowest) for $\Delta\phi = 0$ (c) and $\Delta\phi = \pi$ (d). Lower panels: the width of the Gaussian fit at t_* versus $\Delta\phi$ (e) including mean-field result (red-dashed) and TWA averaged over 200 realizations (black-solid). Overall peak density n_{peak} is shown in panel (f) with lines as in (e). In (e, f) the sampling error of the stochastic averaging is indicated with dotted lines.

In the attractive case, the width of the Gaussian fit, σ_{fit} , is given by the single narrow solitonic peak (figure 4(a)), whereas in the repulsive case it is set by the separation between the solitons, which is much larger (figure 4(b)). A second distinguishing feature is the peak density at the moment of closest approach, which is also the peak density during the collision $n_{\text{peak}} = \max_{x,t} |\Phi(x,t)|^2$. The dependence of both these indicators on the relative phase $\Delta\phi$ is shown in figures 4(e) and (f). In the mean-field treatment they behave as expected, i.e. there is a clear increase in σ_{fit} around $\Delta\phi = \pi$. However, the situation becomes completely different if the effects of vacuum fluctuations on these collisions are accounted for.

We find that in the presence of noise the relative phase between the solitons in the mean-field component of the condensate wave function loses its significance. When averaged over 200 realizations of the atom-field with different realizations of noise, the overall peak of the density, n_{peak} , and the width of the Gaussian fit, σ_{fit} , are no longer distinct for in-phase and out-of-phase

solitons¹⁰. Instead, both variables are *independent* of the initial relative phase. For all relative phases, the width of the Gaussian fit corresponds closely to that of the *repulsive* mean-field simulations.

5. 3D BSW collisions

Finally, we investigate whether observations regarding soliton interactions in the 1D simulations carry over to 3D collisions of BSWs. As stated earlier, full simulations of the entire collapse experiment are numerically intractable. It is possible, however, to study binary collisions of 3D BSWs using the GPE [10, 22]. We extend the work of [10, 22] by performing the same simulations incorporating quantum noise in the TWA, as well as the effects of three-body loss. It has previously been shown in [22] that collisions of BSWs in attractive BECs depend on the collision velocity. In particular, at low velocities a phase difference $\Delta\varphi = \pi$ can increase the possible number of repeated collisions before a significant degradation of the soliton shape. In this section, we show that quantum and thermal noise have the opposite effect, reducing the number of collisions with preserved soliton shape.

Our initial binary soliton state is chosen to most closely fit our findings of section 2. Thus, we employ $K_3 = 2 \times 10^{-40} \text{ m}^6 \text{ s}^{-1}$, an initial total atom number $N_{\text{ini}} = 3500$ and a soliton separation of about $d = 32 \mu\text{m}$ for $a_{\text{collapse}} = -11.4a_0$. We find the initial soliton state using a conjugate gradient method, while neglecting the axial trap. For the dynamical simulation, two replicas of it are symmetrically placed around the origin on the z -axis with a relative phase $\Delta\varphi$. The axial trap is then switched on and the solitary waves are allowed to propagate towards the origin to collide [10, 22].

We determine the remnant atom number of such a scenario after the evolution time of 3 s (as in the experiment of Cornish *et al* [12]). Three theoretical approaches were employed for the dynamical evolution: mean-field theory, truncated Wigner formalism with initial noise only and TWA with the addition of dynamical noise [20]. All simulations use the harmonic oscillator basis. The results are summarized in figure 5. It can be seen that for both initial phases the atom number remaining after 3 s exceeds the critical number¹¹, which for this scenario is $N_{\text{crit}} \approx 2800$. Furthermore, in the presence of three-body loss (figures 5(c) and (e)) the relative phase $\Delta\varphi = \pi$ allows oscillations of the BSW pair in the trap for longer times than $\Delta\varphi = 0$, as was shown without the inclusion of three-body loss in [22].

The inclusion of vacuum fluctuations via the truncated Wigner simulation does not significantly alter the remnant atom numbers around 3 s. It does, however, strongly affect the spatial BSW evolution. As shown in figure 5(g), even for $\Delta\varphi = \pi$ the two clearly separated clouds no longer survive at long evolution times, in contrast to mean-field studies (figure 5(e)). This also disagrees with the experimental results, which did observe BSW-like structures after 3 s and more than 40 collisions between the two wavepackets [12].

Therefore, from our 3D simulations results we cannot conclude that the quantum noise renders BSW collisions more repulsive—in fact quantum noise appears to destabilize the case of $\Delta\varphi = \pi$. We note, however, that this qualitative difference between 3D and 1D results could

¹⁰ In detail, we first obtain σ_{fit} and n_{peak} from each trajectory and *then* take the average. Although this does not have a direct interpretation within the TWA, it provides an indication of how individual experimental realizations might behave and serve as a measure of the effect of quantum fluctuations on the soliton collisions.

¹¹ The critical number is $N_{\text{crit}} = k\bar{a}/|a_s|$, with $k = 0.55$, $\bar{a} = \sqrt{\hbar/m\bar{\omega}}$, $\bar{\omega} = (\omega_r^2\omega_z)^{1/3}$ [12].

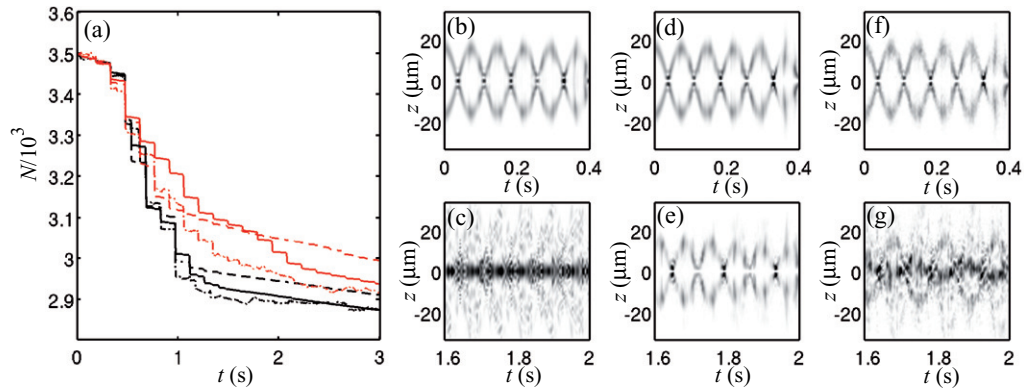


Figure 5. Binary collisions of 3D BSWs under the influence of three-body loss (compare with figure 4 of [10] for corresponding data without three-body loss). (a) Total number of atoms remaining in the trap: mean-field theory (solid), TWA with initial noise (dashed) and TWA with dynamical noise (dot-dashed). Results for different relative phases are shown: $\Delta\varphi = 0$ (black, lower curves), $\Delta\varphi = \pi$ (red, upper curves). Panels (b–g) display atomic density along the z -axis with upper (lower) panels showing the evolution at early (late) times. We present mean-field simulations (b–e) and TWA with initial noise (f, g). The BSWs are in-phase $\Delta\varphi = 0$ (b, c) or out-of-phase $\Delta\varphi = \pi$ (d–g). For BSWs within the single trajectory TWA, we enforce the relative phase before quantum fluctuations are added. Darker areas correspond to higher densities. Note that for better visibility a nonlinear grey scale that exaggerates low density regions is used.

stem from the reduced amount of noise that we are forced to apply in 3D due to numerical reasons¹². The apparent agreement between mean-field theory and the experimental results in [22] is compelling; however, there is no obvious mechanism for the development of the π phase difference, and we can offer no explanation for why a calculation that we expect to be more accurate than GP simulation gives results that so obviously differ from observations in the lab.

6. Conclusions

We have studied the short and long time dynamics of the collapse of attractive BECs, applying 3D and effective 1D models that include three-body losses and quantum noise. We find that due to the kinetic energy liberated, the condensate exhibits violent oscillations in the trap after the collapse, with an amplitude that strongly depends on three-body loss rates, K_3 . We propose that the sensitivity of these oscillations after the collapse may improve measurements of K_3 . After the collapse highly excited BSW-like structures form from the remnant condensate. These also exhibit violent dynamics and disappear, and reform multiple times throughout the evolution.

¹² Care must be taken when interpreting these simulations as quantum field evolution in the sense of the TWA. Due to the application of noise to a restricted set of modes and, in particular, the long evolution times, the TWA is not strictly justified. Nonetheless, the noise present in the simulation can closely mimic the effect of hot uncondensed atoms that are known to be present after the condensate collapse. In this sense we would expect the simulations with noise to offer a more realistic description than a pure GP treatment.

The relative phase between dynamically formed BSWs does not usually take repulsive values ($\pi/2 < \Delta\varphi < 3\pi/2$) as has been previously postulated [12]. However, we show in 1D that the addition of quantum fluctuations can render interactions repulsive, even for solitons with a phase relationship for which standard GP theory predicts them to exhibit attractive interactions. Our 3D studies of interactions with quantum noise do *not* show a similar effect at our level of approximation; instead they suggest that quantum noise results in a shorter BSW lifetime.

Our results raise questions about the interpretation of the JILA and Rice collapse experiments [4, 12] in terms of the creation of BSWs with mutually repulsive relative phases. In light of this, we suggest that the system warrants further theoretical and experimental study. In particular, it will be interesting to compare the results of the present studies with more direct treatments of quantum effects in soliton or BSW collisions. Experimentally, one could aim to measure the soliton phase directly [42] rather than inferring it from collisional behaviour.

Acknowledgments

We thank Simon Cornish, Andy Martin, Nick Parker and Joachim Brand for helpful discussions and comments and Simon Cornish for the provision of the experimental data. This research was supported by the Australian Research Council Centre of Excellence for Quantum-Atom Optics and ARC Discovery Project DP0343094. We also thank the Queensland Cyber Infrastructure Foundation for providing computation resources at the National Facility of the Australian Partnership for Advanced Computing. BJDW is grateful for the hospitality of the Max-Planck Institute for the Physics of Complex Systems in Dresden.

References

- [1] Dalfovo F, Giorgini S, Pitaevskii L P and Stringari S 1999 Theory of Bose–Einstein condensation in trapped gases *Rev. Mod. Phys.* **71** 463
- [2] Kivshar Y S and Agrawal G P 2003 *Optical Solitons: From Fibers to Photonic Crystals* (San Diego, CA: Academic)
- [3] Khaykovich L, Schreck F, Ferrari G, Bourdel T, Cubizolles J, Carr L D, Castin Y and Salomon C 2002 Formation of a matter-wave bright soliton *Science* **296** 1290
- [4] Strecker K E, Partridge G B, Truscott A G and Hulet R G 2002 Formation and propagation of matter-wave soliton trains *Nature* **417** 150
- [5] Eiermann B, Anker T, Albiez M, Taglieber M, Treutlein P, Marzlin K-P and Oberthaler M K 2004 Bright Bose–Einstein gap solitons of atoms with repulsive interaction *Phys. Rev. Lett.* **92** 230401
- [6] Dodd R J, Edwards M, Williams C J, Clark C W, Ruprecht P A and Burnett K 1996 Role of attractive interactions on Bose–Einstein condensation *Phys. Rev. A* **54** 661
- [7] Donley E A, Claussen N R, Cornish S L, Roberts J L, Cornell E A and Wieman C E 2001 Dynamics of collapsing and exploding Bose–Einstein condensates *Nature* **412** 295
- [8] Bradley C C, Sackett C A and Hulet R G 1997 Bose–Einstein condensation of lithium: observation of limited condensate number *Phys. Rev. Lett.* **78** 985
- [9] Gerton J M, Strekalov D, Prodan I and Hulet R G 2000 Direct observation of growth and collapse of a Bose–Einstein condensate with attractive interactions *Nature* **408** 692
- [10] Parker N G, Martin A M, Cornish S L and Adams C S 2008 Bright solitary waves of trapped atomic Bose–Einstein condensates *Physica D* at press doi:10.1016/j.physd.2008.07.001 (arXiv:0802.4275v1)
- [11] Parker N G, Cornish S L, Adams C S and Martin A M 2007 Bright solitary waves and trapped solutions in Bose–Einstein condensates with attractive interactions *J. Phys. B: At. Mol. Opt. Phys.* **40** 3127

- [12] Cornish S L, Thompson S T and Wieman C E 2006 Formation of bright matter-wave solitons during the collapse of attractive Bose-Einstein condensates *Phys. Rev. Lett.* **96** 170401
- [13] Strecker K E, Partridge G B, Truscott A G and Hulet R G 2003 Bright matter wave solitons in Bose-Einstein condensates *New J. Phys.* **5** 73
- [14] Khawaja U A, Stoof H T C, Hulet R G, Strecker K E and Partridge G B 2002 Bright soliton trains of trapped Bose-Einstein condensates *Phys. Rev. Lett.* **89** 200404
- [15] Leung V Y F, Truscott A G and Baldwin K G H 2002 Nonlinear atom optics with bright matter-wave soliton trains *Phys. Rev. A* **66** 061602
- [16] Gordon J P 1983 Interaction forces among solitons in optical fibers *Opt. Lett.* **8** 596
- [17] Timmermans E, Tommasini P, Hussein M and Kerman A 1999 Feshbach resonances in atomic Bose-Einstein condensates *Phys. Rep.* **315** 199
- [18] Savage C M, Robins N P and Hope J J 2003 Bose-Einstein condensate collapse: a comparison between theory and experiment *Phys. Rev. A* **67** 014304
- [19] Wüster S, Hope J J and Savage C M 2005 Collapsing Bose-Einstein condensates beyond the Gross-Pitaevskii approximation *Phys. Rev. A* **71** 033604
- [20] Wüster S, Dąbrowska-Wüster B J, Bradley A S, Davis M J, Blakie P B, Hope J J and Savage C M 2007 Quantum depletion of collapsing Bose-Einstein condensates *Phys. Rev. A* **75** 043611
- [21] Saito H and Ueda M 2000 Intermittent implosion and pattern formation of trapped Bose-Einstein condensates with an attractive interaction *Phys. Rev. Lett.* **86** 1406
- [22] Parker N G, Martin A M, Cornish S L and Adams C S 2008 Collisions of bright solitary matter waves *J. Phys. B: At. Mol. Opt. Phys.* **41** 045303
- [23] Carr L D and Brand J 2004 Spontaneous soliton formation and modulational instability in Bose-Einstein condensates *Phys. Rev. Lett.* **92** 040401
- [24] Steel M J, Olsen M K, Plimak L I, Drummond P D, Tan S M, Collet M J, Walls D F and Graham R 1998 Dynamical quantum noise in trapped Bose-Einstein condensates *Phys. Rev. A* **58** 4824
- [25] Sinatra A, Lobo C and Castin Y 2001 Classical-field method for time dependent Bose-Einstein condensed gases *Phys. Rev. Lett.* **87** 210404
- [26] Sinatra A, Lobo C and Castin Y 2002 The truncated Wigner method for Bose-condensed gases: limits of validity and applications *J. Phys. B: At. Mol. Opt. Phys.* **35** 3599
- [27] Kagan Y, Muryshev A E and Shlyapnikov G V 1998 Collapse and Bose-Einstein condensation in a trapped Bose gas with negative scattering length *Phys. Rev. Lett.* **81** 933
- [28] Roberts J L, Claussen N R, Cornish S L and Wieman C E 2000 Magnetic field dependence of ultracold inelastic collisions near a Feshbach resonance *Phys. Rev. Lett.* **85** 728
- [29] Ueda M and Saito H 2003 A consistent picture of a collapsing Bose-Einstein condensate *J. Phys. Soc. Japan* **72** (Suppl. C)127
- [30] Cornish S L private communication
- [31] Milstein J N, Menotti C and Holland M J 2003 Feshbach resonances and collapsing Bose-Einstein condensates *New J. Phys.* **5** 52
- [32] Santos L and Shlyapnikov G V 2002 Collapse dynamics of trapped Bose-Einstein condensates *Phys. Rev. A* **66** 011602
- [33] Blakie P B and Davis M J 2005 Projected Gross-Pitaevskii equation for harmonically confined Bose gases at finite temperature *Phys. Rev. A* **72** 063608
- [34] Norrie A A, Ballagh R J and Gardiner C W 2006 Quantum turbulence and correlations in Bose-Einstein condensate collisions *Phys. Rev. A* **73** 043617
- [35] Polkovnikov A 2003 Evolution of the macroscopically entangled states in optical lattices *Phys. Rev. A* **68** 033609
- [36] Blakie P B, Bradley A S, Davis M J, Ballagh R J and Gardiner C W 2008 Dynamics and statistical mechanics of ultra-cold Bose gases using *c*-field techniques *Adv. Phys.* **57** 363
- [37] Gardiner C W and Zoller P 2004 *Quantum Noise* 3rd edn (Berlin: Springer)

- [38] Norrie A A, Ballagh R J, Gardiner C W and Bradley A S 2006 Three-body recombination of ultracold Bose gases using the truncated Wigner method *Phys. Rev. A* **73** 043618
- [39] Bao W Z, Ge Y Y, Jaksch D, Markowich P A and Reishauptl R M 2007 Convergence rate of dimension reduction in Bose-Einstein condensates *Comput. Phys. Commun.* **177** 832
- [40] Andersen D and Lisak M 1995 Bandwidth limits due to incoherent soliton interaction in optical-fiber communication systems *Phys. Rev. A* **32** 2270
- [41] Stegeman G and Segev M 1999 Optical spatial solitons and their interactions: universality and diversity *Science* **286** 1518
- [42] Li W 2008 Directly determining the relative phase of two coherent solitary waves in attractive Bose-Einstein condensates arXiv:0805.0260v1